Hindawi
International Journal of Antennas and Propagation
Volume 2019, Article ID 3837190, 16 pages
https://doi.org/10.1155/2019/3837190

Research Article

Measurement Stand and Methodology for Research of the Off-Body and Body-to-Body Radio Channels in WBANs with Different Diversity Schemes

Slawomir J. Ambroziak

Faculty of Electronics, Telecommunications and Informatics, Gdansk University of Technology, 80-233 Gdansk, Poland

Correspondence should be addressed to Slawomir J. Ambroziak; slawomir.ambroziak@pg.edu.pl

Received 4 November 2018; Revised 26 December 2018; Accepted 9 January 2019; Published 9 April 2019

Academic Editor: Renato Cicchetti

The concept of an experimental test bed for system loss and channel impulse response measurements for off-body and body-to-body radio channels in wireless body area networks (WBANs) is fully described. The possible measurement scenarios that may occur in investigation of off-body and body-to-body channels are classified and described in detail. Additionally, an evaluation is provided of the standard and expanded uncertainties of the presented measurement stand and methodology. Finally, the exemplary results are presented and discussed, in order to point out the need for further investigations of different diversity schemes and their applications in WBANs.

1. Introduction

Modern telecommunication technologies and their rapid development cause important changes in the ways humans communicate, as well as changes in communication between humans and machines. In addition, wireless technologies provide independent telecommunication services based on the existence of fixed infrastructure, which results in an improvement of the quality and comfort of human life. Due to the unceasing miniaturization of electronic devices and the simultaneous decrease of their energy consumption, there is an increasing demand for wireless solutions for exchanging information between devices working in close proximity to the human body or even inside it. This kind of short-range radio network, known as the WBAN, was proposed for the first time in 1996 by Zimmermann, who demonstrated the possibility of transmission between two devices using the human body as a transmission medium [1]. The first normalization approach was provided 16 years later in [2].

Due to the ability to integrate various portable or wearable devices with a fixed infrastructure, WBANs will play a significant role in the next generation of radio communication systems, including 5G [3]. The radio channel in WBANs is significantly different from that in traditional radio communication networks, due to the direct proximity of the human body and its movement. Additionally, because of the large diversity of radio link types and the large number of possible scenarios that may occur in WBANs and considering that this area of research is relatively new, it is necessary to thoroughly understand the propagation conditions to enable designing of such networks with high reliability. Therefore, modeling of radio channels is a key issue for the proper operation of WBAN networks and has an impact on the designing of antennas, communication protocols, and transceiver devices.

Empirical models, except for deterministic ones, are one possible way to model radio channel characteristics such as average system loss with slow and fast fading distributions or channel impulse response. In order to build a reliable empirical channel model, it is necessary to perform a comprehensive measurement campaign considering the different places of the antennas' installation, user motion scenarios, different environments, etc. It is also well known that by using different diversity schemes, the quality of transmission may be improved, and thus, this kind of technique should be also considered in measurement research of radio channel

characteristics. Such research works are carried out within the COST Action CA15104 "Inclusive Radio Communication Networks for 5G and beyond" (IRACON) [4]. The general methodology for measurements of radio channels with space and polarization diversity schemes has been presented in the article.

Currently, there are only few studies dealing with experimental investigations of radio channels with space diversity schemes that also describe the measurement methodology and scenarios. Space diversity in an off-body channel at 2.45 GHz has been considered in [5, 6], specifically the transmit diversity in the former and the reception diversity in the latter. Measurement equipment and selected scenarios for space diversity in on-body channels at the same frequency band have been presented in [7, 8]. On the other hand, in [9], a testbed has been presented that may be used for polarization diversity measurements in off-body channels. In [10, 11], one can find description of experimental facilities and scenarios for on-body channels at 2.45 GHz that can be used for analysis of correlation between signals received by two antennas placed in different positions on the body. In the literature, there are also papers containing descriptions of measurement stands for simple Single Input Single Output (SISO) channels, e.g., on-body channels at ultrawideband (UWB) frequencies [12–14], off-body channels at 868 MHz [15], or body-to-body channels for UWB and ISM bands [16, 17]. To the best of the author's knowledge, there are no papers describing a versatile measurement stand and methodology for comprehensive investigations of off-body and body-to-body radio channels in WBANs with space and polarization diversity schemes. Thus, the aim of this article is to fill this gap.

The rest of the article is structured as follows. Section 2 describes the concept of the versatile experimental setup for system loss and channel impulse response measurements. Section 3 deals with the classification of measurement scenarios that should be considered in WBAN investigations. Section 4 presents the evaluation of the standard and expanded uncertainty of the presented measurement stand and methodology. Section 5 shows the exemplary results of system loss and channel impulse response measurements for space and polarization diversities. Analysis of these results leads to the conclusion that there is a need for further investigation of different diversity schemes in WBANs.

2. Concept of the Versatile Measurement Stand

The block diagram of the versatile measurement stand for radio channel measurements in WBANs with space and polarization diversity schemes is presented in Figure 1. The stand consists of four functional parts: control section (CS), executive section (ES), RF switching section, and antennas' section (AS).

2.1. Executive Section. The ES is divided into two independent parts that can be used depending on the type of radio channel parameters that one needs to measure, i.e., system loss (SL) or channel impulse response (CIR). For the former, one can use the transmitting (Tx) and receiving (Rx) parts. This solution allows for any deployment of Tx and Rx in the environment as well as investigation of longer radio links without significant influence of the RF cables' attenuation. The Tx part consists of a vector signal generator (VSG) SMU 200A that allows generation of any RF signal at a frequency from 100 kHz up to 6 GHz. It is noteworthy that after hardware extensions, it could be possible to generate two independent RF signals, e.g., for transmitting diversity or MIMO measurements. The Rx part consists of two digital wideband R&S EM550 receivers that can be used for investigations of space diversity or polarization diversity, depending on the antenna set being used. It should be noted that the average time between particular measurements of received signal powers is around 3 ms. Before measurements, both the Tx part and the Rx part should be calibrated.

In the part responsible for CIR measurements, the Agilent E5071C vector network analyzer (VNA) is used. It allows for measurements in the frequency band from 300 kHz up to 20 GHz. While the measurements are always done in the frequency domain, the results provided by the VNA may be given directly in the time domain, or in the frequency domain, and then, CIR can be calculated in postprocessing. The main parameters that have to be set up are the center frequency, the bandwidth, the power transmitted by port 1, and the number of points. The value of the intermediate frequency filter bandwidth (IF bandwidth), which is a key factor in the selectivity of the VNA, should be chosen in order to ensure that the noise level is not larger than a certain value. For example, for a center frequency of 5.8 GHz, bandwidth of 500 MHz, Tx power of 0 dBm, and an IF bandwidth of 70 kHz, the maximum noise level equals -103 dBm, with an average of -111 dBm. Before measurements, the VNA should be calibrated. It should be also stressed that the narrower IF bandwidth causes a longer time requirement for a single measurement.

2.2. RF Switching Section. In order to carry out measurements with different diversity schemes, there is a need to switch RF inputs of the digital receivers (SL measurements) or ports 2 and 3 of the VNA (CIR measurements) between the two types of antenna sets in the AS. The switching mechanism may be manual or automatic. In the first case, the RF connections between ES and AS are configured manually by use of the RF cables. In the case of an automatic mode, remotely controlled electromechanical switches should be used, e.g., Tesoel TS121. In this case, the certain configuration of RF switches is set by the CS via an RS232 interface. The connections between the RF switching section and AS should be realized using a flexible, high-frequency, and high-quality cable, e.g., Sucoflex 126E, that allows for precise measurements with high phase stability combined with low loss and good return loss up to 26.5 GHz.

2.3. Antennas' Section. Depending on the scenario, the Tx antenna may be considered as an off-body or on-body antenna. In the first case, one can use a UWB omnidirectional antenna, e.g., OA2-0.3-10.0 V/1505, designed for operation in the frequency range of 0.3–10.0 GHz. In the case of an on-body antenna, one should remember that during

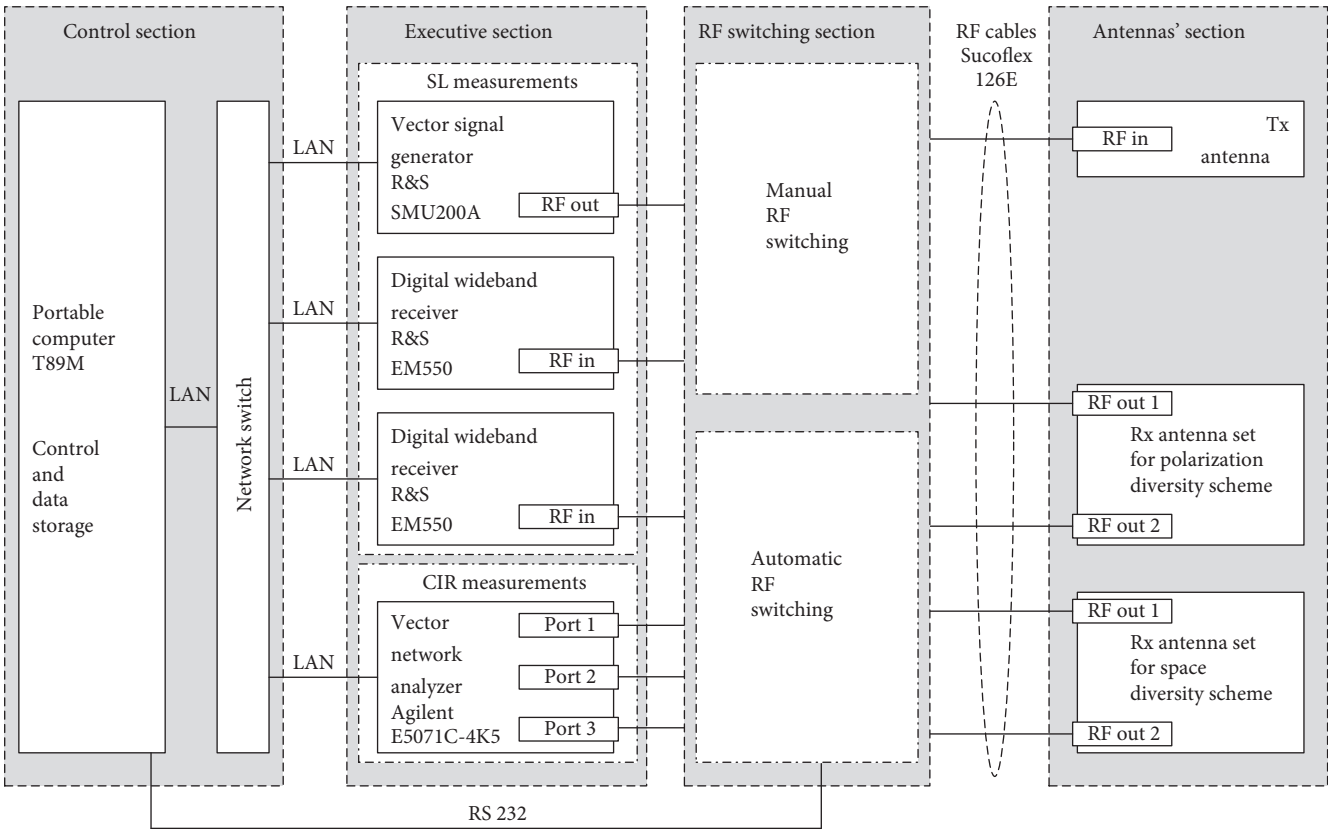

Figure 1: The block diagram of the versatile measurement stand for radio channel measurements in WBANs with space and polarization diversity schemes.

design of this type of antenna, the influence of the human body on the antenna parameters should be considered. An example of such an antenna may be the linearly polarized UWB monopole antenna, described in [18], designed to work in the frequency band between 3 GHz and 10 GHz, or as described in [19], a dual-band WLAN belt antenna designed for WLAN in industrial, scientific, and medical (ISM) bands at 2.45 GHz and 5.8 GHz.

Similarly, the Rx antenna set can also be placed on the user's body or in some external location. Considering the polarization diversity and the off-body case, one can use a dual-polarized antenna, e.g., the quad-ridged horn antenna LB-OSJ-0760, designed for operation in the frequency range of 0.7–6 GHz [20]. In the case of an on-body Rx antenna for polarization diversity, one can use a dual-polarized UWB antenna designed to work in the frequency band between 3 GHz and 10 GHz [21] or a dual-polarized dual-band WLAN antenna designed for ISM bands at 2.45 GHz and 5.8 GHz [22]. In contrast, if we consider a space diversity scheme, one can use two antennas of any kind, e.g., the coplanar-fed ultrawideband monopole antennas, or even two simple rectangular patch antennas.

2.4. Control Section. The CS consists of a portable computer (e.g., a Mecer Toughbook T89 M with Intel Atom Z530) responsible for controlling the work of the whole measurement stand and collecting measurement data and a network switch that allows for control of four devices via a LAN interface at the same time. Communication between the CS and ES is realized using the National Instruments implementation of the Virtual Instrument Software Architecture (NI-VISA) standard and Standard Commands for Programmable Instruments (SCPI).

The principle of measurement stand operation in configuration for SL measurements has been presented as a simplified algorithm for control software (see Figure 2). After connecting with both receivers, the configuration parameters are read and sent to them. In the next step, the output file is created, and the system waits for the start of the measurements. Before that, it is recommended to turn the RF output on. After measurements start, the portable computer connects with the generator and reads and sends the configuration parameters to it.

Depending on the "stop mode" set in the application configuration, there are three possible modes of measurements. The first mode is a manual stop mode, in which the measurements are done in a loop until the stop button is pressed. The second mode is a sample size mode, in which a specific number of measurements are performed. The last mode is a sample time mode, in which measurements are completed by a specified time period. Regardless of the mode, a single measurement is done by triggering the power measurement in each receiver and reading the received value. After that, the system loss values are calculated basing on the measured

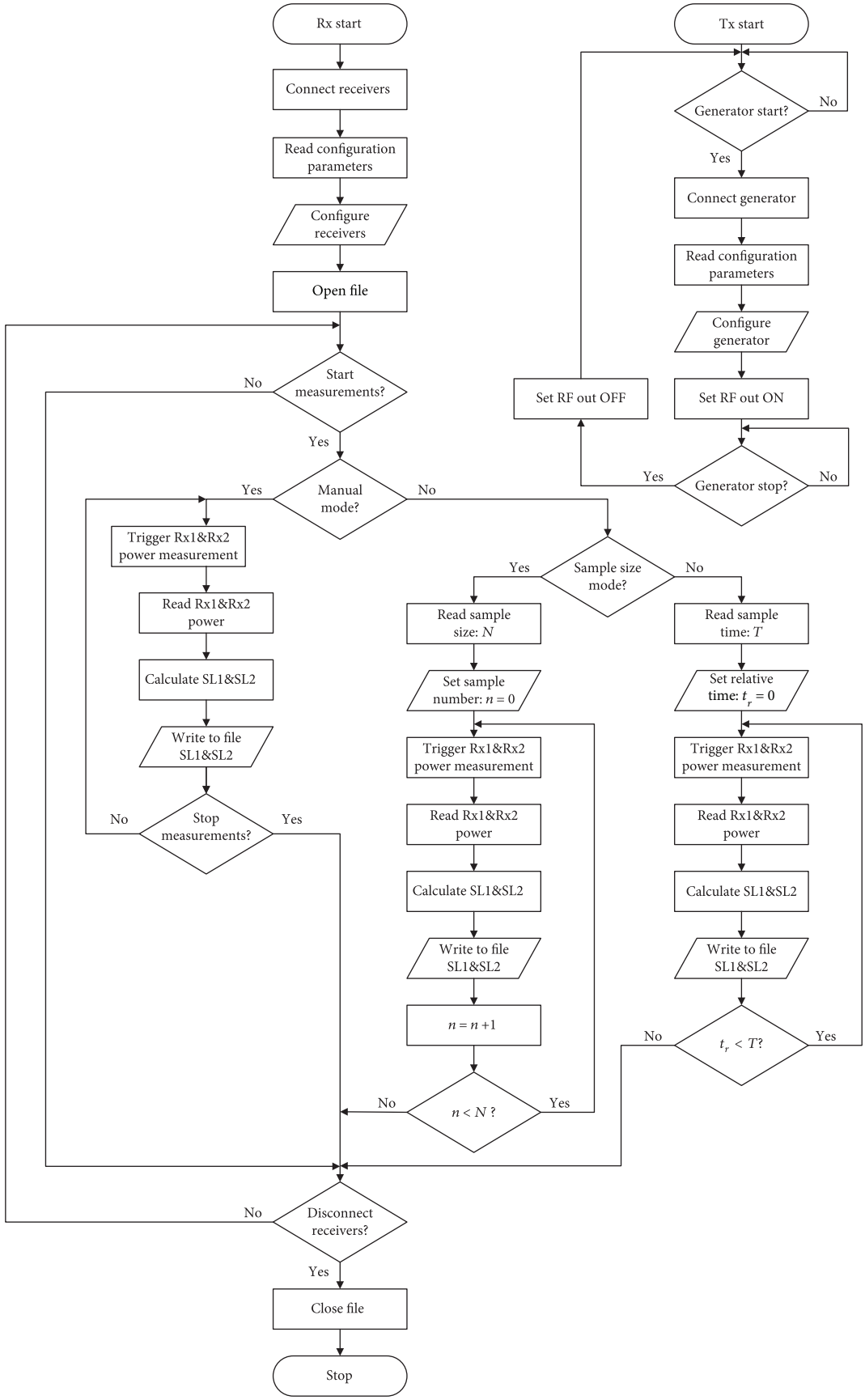

Figure 2: Simplified algorithm of control software for performing system loss measurements.

power value, transmitted power, and attenuation values of the Tx and Rx cables. After finishing the measurements, the user can disconnect the receivers and close the file with results, but there is also a possibility of repeating the measurements many times, writing the results to the same file.

A simplified algorithm of control software for performing CIR measurements has been presented in Figure 3. After starting the application, the software waits for connection with the VNA. When the connection is set up, the text file for measurement data storage is opened, and the application waits for confirmation of proper calibration of the VNA. It should be done and confirmed manually by the user. After that, the test bed is ready for measurements. Similar to the SL measurements, there are three possible modes for measurement termination. The single measurement consists of its triggering, reading the measured CIR, and writing it to the output file. After finishing the measurements, the user can disconnect the VNA and close the file with results, but there is also a possibility of repeating the measurements many times, writing the results to the same file.

3. Classification of Measurement Scenarios

A very important part of measurement methodology is establishing a proper measurement scenario. One has to know what kind of information to obtain about the radio channel. The right selection of the environment, the type of user motion, and the location of the antenna are of equal importance. As such, the scenarios that may occur in off-body and body-to-body networks have been classified and are presented in Figure 4. It should be noted that this is not a closed list, and it may be changed or updated according to the goals of research.

3.1. Object of Measurements. The measurement stand presented in the previous section allows for measurements of SL or CIR depending on its configuration. The parameters used in the exemplary result analysis are presented in the following part of the paper.

The system loss (L_s) is defined in [23] as the difference (expressed in dB) between the RF power input to the terminals of the transmitting antenna (P_{Tx}) and the resultant RF signal power available at the terminals of the receiving antenna (P_{Rx}) and can be expressed by

$$L_{s[dB]} = P_{Tx[dBm]} - P_{Rx[dBm]}. \quad (1)$$

In addition, while analyzing polarization diversity, based on the SL measurements for orthogonally polarized Rx antennas, it is possible to calculate the cross-polarization discrimination (XPD), which is the most common metric used to characterize depolarization properties of wireless channels. The XPD (in a linear domain) may be calculated as the ratio between the Rx powers received in the copolarized (CP) and cross-polarized (XP) channels [24], p_r^{CP} and p_r^{XP}, respectively. Additionally, for a given vertical linear polarization of the Tx antenna, XPD can be obtained from the system loss values observed in the XP and CP channels [9] as

$$XPD_{[dB]} = 10 \log \left(\frac{p^{CP}_{r[W]}}{p^{XP}_{r[W]}} \right) = L^{H}_{s[dB]} - L^{V}_{s[dB]}, \quad (2)$$

where the superscripts H and V indicate the horizontal and vertical polarizations, respectively.

The CIR, $h(t, \tau)$, is commonly used for characterization of the multipath channels using a power delay profile (PDP), which can be calculated as the square of the amplitude of the CIR, $|h(t, \tau)|^2$. The described measurement stand allows for measurements of the instantaneous PDP, which is defined as the power density of the impulse response at one moment and at one point [25]. There are a number of statistical parameters that can be calculated based on CIR, and all of them are well described in literature, e.g., [25]. Only selected parameters have been briefly presented here. The first one is the total power (in the linear domain) of CIR, p_r, which can be calculated from the power density of CIR, $p(t)$, according to the following formula [25]:

$$p_r = \int_{t_F}^{t_L} p(t)dt, \quad (3)$$

where $p(t)$ is power density of CIR in the linear domain, t is delay with respect to a time reference, t_F is time for which $p(t)$ exceeds the certain cut-off level for the first time, and t_L is time for which $p(t)$ exceeds the certain cut-off level for the last time.

The next parameter is the number of multipath components, which is defined as the number of peaks in a PDP whose amplitude is not lower than the certain value from the highest peak and above the noise floor. The third statistic is the average delay, μ_τ, which is defined as the power-weighted average of the excess delays, and is given by the first moment of the PDP [25]:

$$\mu_\tau = \left[\frac{\int_0^{t_L - t_F} \tau p(\tau) d\tau}{\int_0^{t_L - t_F} p(\tau) d\tau} \right] - \tau_a, \quad (4)$$

where τ is excess time delay (equals to $t - t_F$) and τ_a is arrival time of the first received multipath component (first peak in the PDP).

The last statistical parameter is the r.m.s. delay spread, σ_τ, which is used in the analysis part, provides a measure of the variability of the mean delay, is defined as the power-weighted standard deviation of the excess delays, and is given by the second moment of the power delay profile, i.e., [25]

$$\sigma_\tau = \sqrt{\frac{\int_0^{t_L - t_F} (\tau - \mu_\tau - \tau_a)^2 p(\tau) d\tau}{\int_0^{t_L - t_F} p(\tau) d\tau}}. \quad (5)$$

It is also noteworthy that the r.m.s. delay spread may be used for calculation of the channel coherence bandwidth with different correlation thresholds, as is described in [26].

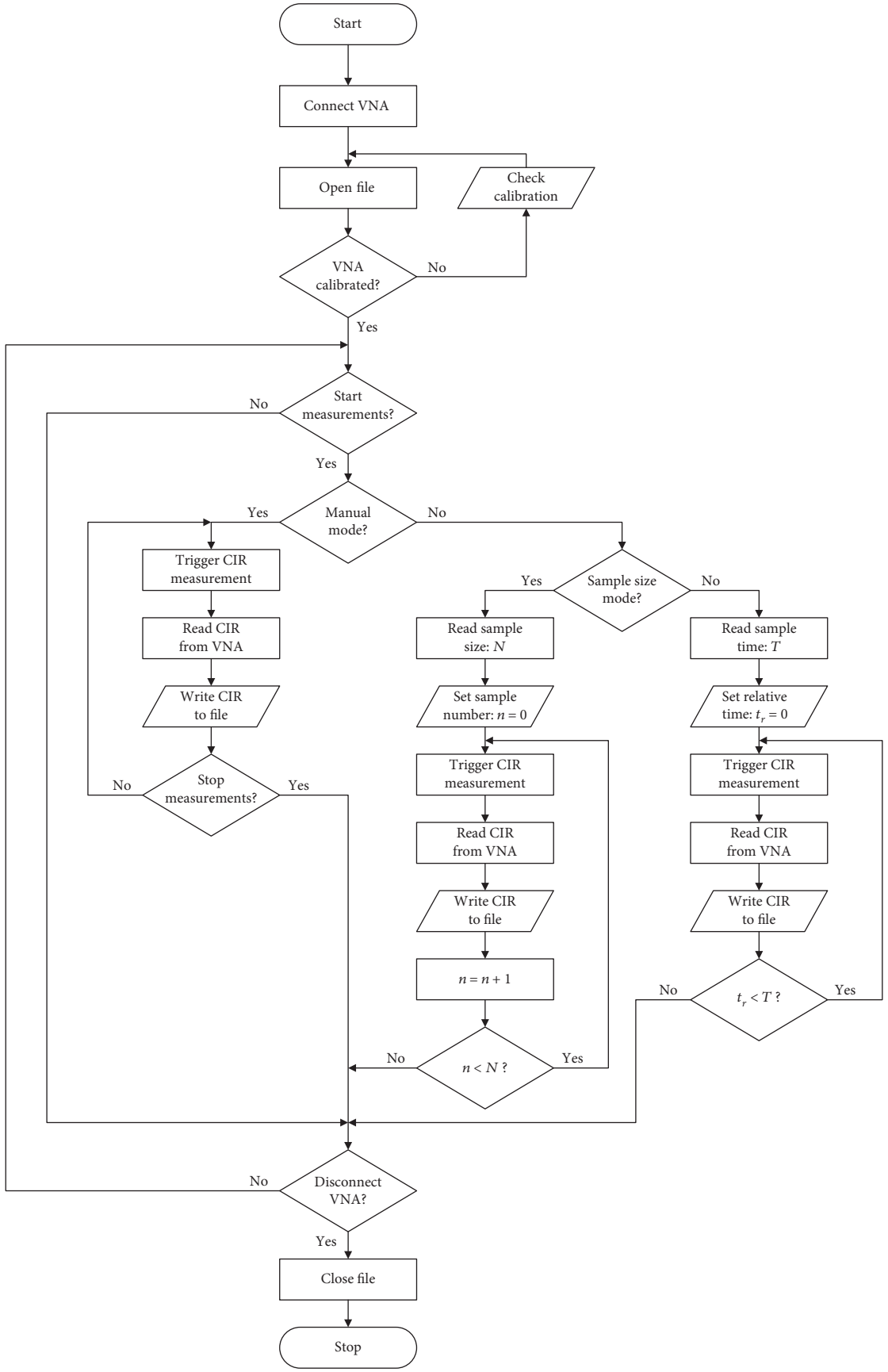

Figure 3: Simplified algorithm of control software for performing channel impulse response measurements.

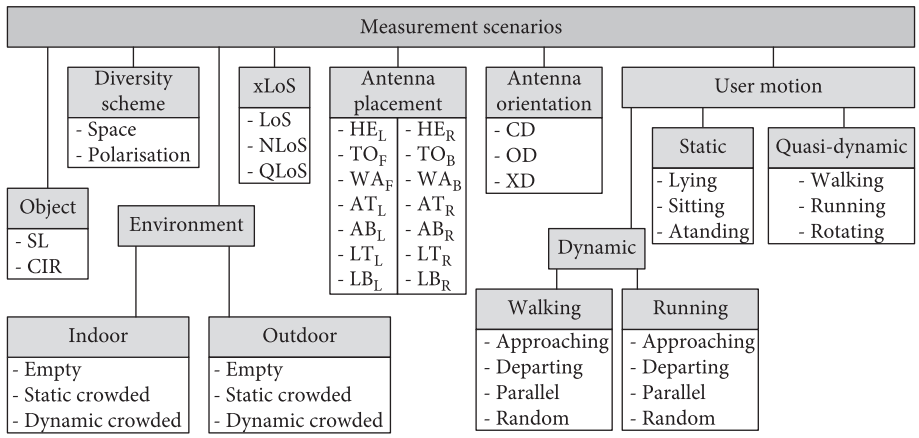

Figure 4: Classification of the measurement scenarios in off-body and body-to-body radio channels.

Taking the above into account, based on the measurement results obtained with the described measurement stand, one can thoroughly characterize a radio channel with space or polarization diversity.

3.2. Diversity Scheme. Reception diversity is a technique in which different independent replicas of the same RF signal propagating through a multipath channel are received and combined in a certain way, in order to minimize the influence of the signal fading. To realize the reception diversity, one has to decorrelate two or more signal replicas and use a well-known combining method, like selection combining, equal-gain combining, or maximal ratio combining [27]. The most commonly used diversity schemes are polarization diversity and space diversity. The described measurement stand allows for measurement scenarios with both.

3.3. Mutual Visibility of Tx and Rx Antennas. While analyzing a measurement scenario, one also has to define the mutual visibility of the Tx and Rx antennas (xLoS in Figure 4). In a case of line-of-sight (LoS), a direct visual line between both antennas exists. When such a line is obstructed by any kind of obstacle, e.g., a wall, furniture, or a human body, the non-line-of-sight (NLoS) conditions occur. The third case, quasi-line-of-sight (QLoS), occurs when the Tx antenna is oriented orthogonally to the Rx antenna, the direct propagation path is either clear or partially obstructed, and the antenna gain is considerably lower than that in the LoS case [28].

3.4. Environment. It is considered that the main applications of WBANs are in healthcare and remote patient monitoring, so the main operating environments seem to be indoor, e.g., a hospital or home. However, this kind of network can also operate in outdoor environment, e.g., in a case of soldiers on the battlefield or remote monitoring of vital signs of football players. Thus, both types of environments should be considered in experimental investigations. In both cases, one can consider an empty environment, i.e., without any other individuals except the WBAN users, or a crowded one, with the influence of nonuser persons. Depending on the behavior of people in the environment, one can distinguish between static (people just standing) or dynamic (people are moving, e.g., walking or gesticulating) crowd scenarios.

3.5. Antenna Placement. The best way to determine the antenna placement is human body segmentation, as it has been proposed in [29] and shown in Figure 5. In order to indicate the wearable antenna placement, one can use the label related to the particular body segment and the orientation. Thus, the most commonly used antenna placements are

(i) left or right side of the head, HE_L or HE_R, respectively

(ii) front or back side of the torso, TO_F or TO_B, respectively

(iii) front or back side of the waist, WA_F or WA_B, respectively

(iv) left or right side of the arm top, AT_L or AT_R, respectively

(v) left or right side of the arm bottom, AB_L or AB_R, respectively

(vi) left or right side of the leg top, LT_L or LT_R, respectively

(vii) left or right side of the leg bottom, LB_L or LB_R, respectively

The selection of a particular antenna placement depends on the planned application of the WBAN being designed.

3.6. Mutual Antenna Orientation. As the system loss strongly depends on the mutual orientation of both antennas in the WBAN radio link, as has been proved in [30], three cases can be considered for the single antenna orientation [31]:

(i) Co-Directed (CD)—when the maximum gain of one antenna is directed towards the other one

(ii) Opposite-Directed (OD)—when the maximum gain of one antenna is directed in the opposite direction to the other one

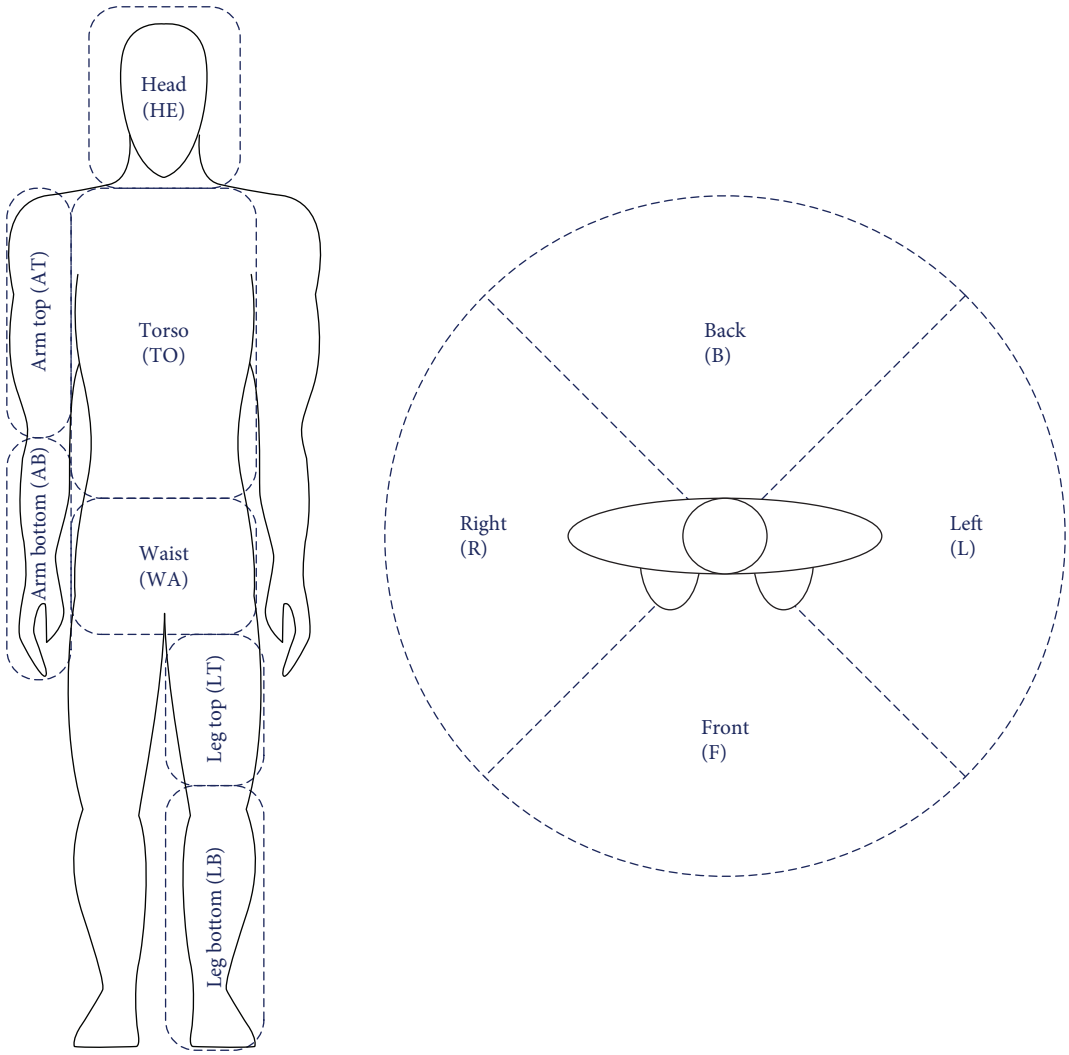

Figure 5: Segmentation and orientation of the human body proposed in [29].

(iii) Cross-Directed (XD)—when the maximum gain of one antenna is directed in an orthogonal direction to the other one

Taking the above into account and considering the mutual orientation of two antennas, one can distinguish the following cases [29, 30]: Co-Co-Directed (CCD), Co-Cross-Directed (CXD), Co-Opposite-Directed (COD), Cross-Cross-Directed (XXD), Cross-Opposite-Directed (XOD), and Opposite-Opposite-Directed (OOD).

3.7. User Motion. Three different scenarios of user motion can be considered during the measurements. The user may be static in the environment with a lying, sitting, or standing position. The user may be also dynamic (walking or running) with four possible directions of motion:

(i) Approaching the external antenna (off-body) or the other user (body-to-body)

(ii) Departing from the external antenna (off-body) or from the other user (body-to-body)

(iii) Parallel motion of two users in the same direction (body-to-body)

(iv) Random motion of user or users in the environment

One can also distinguish a so-called quasi-dynamic scenario, in which the user mimics a particular motion, e.g., walking, running, or rotating in a fixed place.

4. Evaluation of the Measurement Uncertainty

Regardless of the measurement methodology, it is impossible to absolutely determine the exact value of a physical quantity. The difference between the measurement result and the true value of the measured quantity is called the measurement error. One can distinguish between a reading error, a systematic error, and a random error. A reading error usually arises due to inattentiveness or carelessness of the observer in reading or writing results or as a result of a sudden change in measurement conditions (e.g., shocks). This kind of error is easy to detect and remove, if several series of measurements

have been performed. A systematic error results from imperfections of instruments and measurement methods. It can be reduced by using more precise methods and instruments, but it is impossible to completely eliminate this kind of error. Identified systematic error should be taken into consideration by introducing appropriate corrections to the result. The random error is always present in the measurement results. It arises from various accidental and unpredictable factors (e.g., variations of the temperature or reflections of RF signals from a moving object). The existence of random error is demonstrated by the unrepeatability of measurement results of the same physical quantity. This kind of error can be reduced by multiple repetition of the measurements, by which there is a partial compensation for random deviations of the result.

4.1. Standard Uncertainty of Measurement. The international standard [32] recommends using the term "measurement uncertainty" instead of "measurement error." In the standard, the uncertainty of measurement is defined as a parameter that is associated with the result of a measurement and that characterizes the dispersion of the values that could reasonably be attributed to the measurand, i.e., the particular quantity subject to measurement. The measure of measurement uncertainty is the standard uncertainty, defined as the uncertainty of the result of a measurement expressed as a standard deviation. It can be evaluated in two ways: type A—a method of evaluation of uncertainty by statistical analysis of a series of observations (e.g., using experimental standard deviation of the measured values)—and type B—a method of evaluation of uncertainty by means other than the statistical analysis of the series of observations, i.e., based on all of the available information on the possible variability of the measured quantity [32]. This information may include, among others, the manufacturer's specifications, data provided in calibration, and other certificates.

In order to estimate the standard uncertainty of the measurement of a physical quantity X that is performed by this particular measurement stand, one has to use the type B evaluation and consider the above-mentioned data about all equipment that is part of the stand (e.g., antennas, RF cables, and receiver) and other factors that can influence the measurement accuracy, e.g., imperfection of the methodology, or the human factor. One has to note that all factors should be independent and uncorrelated. It may be calculated with the following equation:

$$U_B(X) = \sqrt{\sum_i \left(\frac{U_{B,i}(X)}{d_i}\right)^2}, \tag{6}$$

where $U_B(X)$ is standard uncertainty of the measurement of X, for the measurement stand; $U_{B,i}(X)$ is standard uncertainty of the measurement of X, for the ith factor; and d_i is the coefficient dependent on the distribution of the probability that the measured value of X is within the range of standard uncertainty for the ith factor.

The d_i coefficient equals $\sqrt{3}$ for uniform or rectangular distributions of possible measured values of X within the interval. In case of a normal distribution, this coefficient equals 1.64, 1.96, or 2.58 for a 90%, 95%, or 99% level of confidence, respectively.

4.2. Expanded Uncertainty. If one wants to present the standard uncertainty as an interval around the measurement result, the expanded uncertainty, $U(X)$, should be used. It is a product of the standard uncertainty, $U_B(X)$, multiplied by the so-called coverage factor, k, and can be expressed by

$$U(X) = k \cdot U_B(X). \tag{7}$$

The expanded uncertainty allows for the following notation of measured value: $X \pm U(X)$.

The choice of the coverage factor, k, depends on the required confidence interval, typically in the range from 2 to 3. For the confidence interval of 95%, $k = 2$ should be taken, while for the confidence interval of 99%, $k = 3$ should be taken.

4.3. Uncertainty Estimation for the Versatile Measurement Stand. In order to evaluate the standard uncertainty of the versatile measurement stand, the uncertainties of the following factors have been considered: VSG, VNA, Tx and Rx cables, receivers, methodology imperfection, and the human factor. In Table 1, the expanded uncertainty has been evaluated for a confidence interval of 95%, i.e., for a coverage factor which equals 2. The pessimistic case additionally considers the RF switch (for the automatic RF switching mode), as well as the Tx and Rx antennas. The standard uncertainty equals 2 dB for SL and 1.7 dB for CIR measurements. The expanded uncertainty equals ±4.0 dB and ±3.4 dB, respectively.

Because (according to the SL definition [23]) the antenna is considered as a part of the WBAN radio channel, it is possible to ignore the uncertainty of the antennas' gain. In addition, for the manual RF switching mode, one can also omit the uncertainty of the RF switch. The uncertainty evaluation for this case may be considered as the optimistic case. For SL measurements, the standard uncertainty equals 1.5 dB, while the expanded one equals ±3.0 dB. On the other hand, for CIR measurements, these values are 1.1 dB and ±2.2 dB, respectively.

5. Exemplary Results

The versatile measurement stand and the methodology described in the study have been used to performed complex measurements for different diversity schemes and for different scenarios and environments. In this section, some selected results for off-body channels have been presented, i.e., SL measurements for space diversity in the office and ferry environments, SL measurements for polarization diversity in the ferry environment, and CIR measurements for polarization diversity in the office environment.

5.1. System Loss Measurements for Space Diversity in the Office Environment. Measurement of SL in the office environment has been performed for a narrowband off-body channel at 2.45 GHz. The omnidirectional Cobham OA2-0.3-10.0V/1505, with 2 dBi gain and 65° half-power beamwidth

Table 1: Evaluation of the standard uncertainty and expanded uncertainty for 95% confidence interval ($k = 2$).

Object of measurement	i	Factor	d_i	Pessimistic case			Optimistic case		
				$U_{B,i}$ (dB)	U_B (dB)	U (dB)	$U_{B,i}$ (dB)	U_B (dB)	U (dB)
System loss	1	VSG	$\sqrt{3}$	0.9	2.0	±4.0	0.9	1.5	±3.0
	2	Tx cable		0.2			0.2		
	3	Tx antenna		1.6			—		
	4	RF switch		0.3			—		
	5	Rx antenna		1.6			—		
	6	Rx cable		0.2			0.2		
	7	Receiver		1.5			1.5		
	8	Methodology imperfection		1.0			1.0		
	9	Human factor		1.5			1.5		
Channel impulse response	1	VNA	$\sqrt{3}$	0.5	1.7	±3.4	0.5	1.1	±2.2
	2	Tx cable		0.2			0.2		
	3	Tx antenna		1.6			—		
	4	RF switch		0.3			—		
	5	Rx antenna		1.6			—		
	6	Rx cable		0.2			0.2		
	7	Methodology imperfection		1.0			1.0		
	8	Human factor		1.5			1.5		

in the E-plane, has been used as the Tx antenna and was mounted in the middle of the room at 2.6 m, close to the wall. On the other hand, the Rx antenna set consisted of two linearly polarized wearable patch antennas with 3 dBi gain and half-power beamwidths of 115° and 40° in the H- and E-planes, respectively. The Rx antenna set has been placed on the male user with a height of 1.65 m and a weight of 64 kg. As for the office environment, a conference room with dimensions of 7 m per 5 m and a height of 3 m has been chosen. Nine combinations of the following on-body antennas' placements have been considered: TO_F, TO_B, AB_L, AB_R, HE_L, and HE_R, according to Table 2. The dynamic motion scenario has been selected—the user was walking along the axis of the room ten times for each Rx antenna set configuration [33]. The mean values (μ) and standard deviation (σ) of system loss for different placements of the space diversity Rx antennas have been presented in Table 2.

The absolute difference ($|\delta|$) of SL values obtained for Rx1 and Rx2 has been also presented. One can notice that these differences are from 0.6 dB for the TO_F-AB_L configuration up to 8.7 dB for the TO_B-HE_R one. The obtained average difference is 4.2 dB. These results show that there is a justified need to apply the space diversity scheme in WBANs with off-body communication, in which there is no certainty of the mutual orientation of on-body and off-body antennas. The standard deviation values of SL—being in the range from 6.5 dB to 7.5 dB—are practically independent on the Rx antennas' configuration.

The space diversity scheme may be useful even when the mean SL values are similar, like for the TO_F-AB_L configuration of the Rx antenna set. The magnitudes of fast fading (L_{ff}) for this case, obtained for particular on-body antennas' placements, have been presented in Figure 6. It can be seen that the deep fades (reaching even -40 dB) of the RF signal received by the two antennas do not occur at the same time.

Table 2: The mean (μ) and standard deviation (σ) of system loss for different placements of the space diversity Rx antennas for a walking scenario in the office environment.

Rx no.	Rx antenna placement	μ (dB)	$\lvert\delta\rvert$ (dB)	σ (dB)
Rx1	TO_F	61.6	2.3	7.2
Rx2	TO_B	59.3		7.5
Rx1	TO_F	61.5	0.6	6.7
Rx2	AB_L	60.9		6.9
Rx1	TO_F	61.0	3.3	7.1
Rx2	AB_R	57.7		7.0
Rx1	TO_F	61.5	2.3	7.3
Rx2	HE_L	59.2		7.2
Rx1	TO_F	61.9	7.5	6.5
Rx2	HE_R	54.4		6.8
Rx1	TO_B	64.0	1.8	7.0
Rx2	AB_L	62.2		7.4
Rx1	TO_B	64.2	7.0	7.4
Rx2	AB_R	57.2		7.0
Rx1	TO_B	64.3	4.2	7.2
Rx2	HE_L	60.1		6.9
Rx1	TO_B	63.8	8.7	6.7
Rx2	HE_R	55.1		6.8

5.2. System Loss Measurements for Space Diversity in the Ferry Environment. The SL measurements for space diversity in the ferry environment have been performed for a

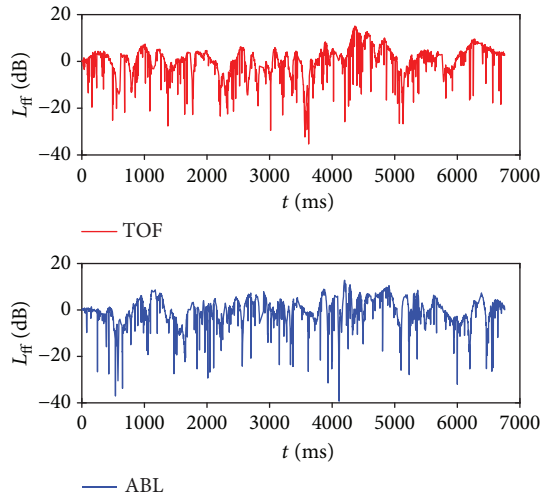

FIGURE 6: Magnitude of fast fading (L_{ff}) vs. time (t) for TO_F-AB_L configuration of the Rx antenna set.

narrowband off-body channel at 2.45 GHz, in a passenger cabin on the M/F Wawel ferry boat running from Poland to Sweden. The cabin's dimensions are 4.4 m per 2.3 m, with a height of 2.1 m. The walls, floor, and ceiling are made of metal. The patch off-body antenna with linear polarization and hemispherical radiation characteristics has been used as a Tx antenna mounted in the middle of the ceiling. The half-power beamwidth equals 115° in the H-plane and 140° in the E-plane. On the other hand, as for the Rx antenna set, two wearable flexible planar inverted F antennas (FlexPIFA [34]) with linear polarization and 2 dBi gain have been used. The performed motion scenario was static, with the user (with a height of 1.72 cm and weight of 60 kg) lying on the lower or upper sleeping berth (also made of metallic material) inside the cabin. The lower berth height is 0.4 m, and the upper berth height is 1.35 m, which gives the distance values between the Tx antenna and berths as 1.2 m and 2 m, respectively, for the upper and lower berths [6]. Three possible placements of the Rx antennas have been considered, namely, TO_F, TO_B, and AB_R. In the study, the following four different lying scenarios have been analyzed:

(i) The user lying on the back with hands along the body

(ii) The user lying on the front with hands under the head

(iii) The user lying on the left side with the right hand under the head

(iv) The user lying on the right side with the right hand under the head

Table 3 presents the mean (μ) and standard deviation (σ) of SL for the upper and lower berths. For the upper berth, the absolute difference ($|\delta|$) of SL values obtained for Rx1 and Rx2 is from the range of 0.2 dB to 10.8 dB, with an average of 7 dB. For the lower berth, these differences are from 1.5 dB up to 13.6 dB, with an average of 6 dB. Therefore, the difference in SL values for the two presented cases is significant, which is beneficial for the use of the diversity scheme.

5.3. System Loss Measurements for Polarization Diversity in the Ferry Environment. The same ferry environment has been investigated in terms of SL measurements in the off-body narrowband channel at 2.45 GHz, with polarization diversity. In this case, a walking scenario has been considered. The measurements have been carried out in a straight corridor with a length of 20 m, a width of 1 m, and a height of 2 m. Most of the construction elements in this environment (i.e., walls, ceiling, doors, and handrails) are made of steel with different thicknesses. The floor is also made of steel but additionally was covered with a covering. The Tx antenna was a linearly polarized wearable patch antenna with 3 dBi gain and half-power beamwidths of 115° and 40°, respectively, in the H- and E-planes. It was mounted on a user with 1.72 m height and 60 kg weight, in three locations: HE_R, TO_F, and AB_L. As for the Rx antenna, the dual-polarized UWB antenna has been used. Its height was 1.3 m above the floor level. Two walking scenarios were realized: the user approaching the Rx antenna and the user departing the Rx antenna. The walking distance was 14 m (from 2 m up to 16 m away from the Rx antenna), and the length of the propagation path of the radio wave was from 0 m up to 16 m. The measurements have been repeated 10 times for each scenario and each antenna placement, in order to obtain a statistically reliable number of measurements.

Table 4 summarizes the mean (μ) and standard deviation (σ) of SL, as well as the average XPD for different polarizations of the Rx antenna. The influence of the Rx antenna polarization on the standard deviation, which is from the range of 6.6 dB to 7.5 dB, is insignificant. According to (2), the XPD is a difference of the power received by Rx2 and Rx1, and one can notice that this difference is from a range of 2.7 dB up to 9.0 dB and is always positive, which shows that on average, the power received by the vertically polarized antenna is higher than that received by the horizontally polarized one.

Nevertheless, considering the local values of XPD as a function of the propagation path length, as shown in Figure 7, it may be seen that negative XPD values may occur. In such a case, the power received by the horizontally polarized antenna may be even 6 dB higher than that for the vertically polarized one. This become an argument for use of polarization diversity in WBANs. Additionally, the comparison of fast fading magnitudes for horizontal and vertical polarizations of the Rx antenna and for the approaching and departing scenarios (see Figure 8) has shown that the deep fades, reaching even -60 dB, do not occur at the same time/place. Thus, by a proper combination of H- and V-polarized signals, one can avoid the consequences of the fast fading phenomenon.

5.4. Channel Impulse Response Measurements for Polarization Diversity in the Office Environment. The CIR measurements for a wideband off-body channel at 5.8 GHz with a polarization diversity scheme have been performed

Table 3: The mean (μ) and standard deviation (σ) of system loss for different placements of the space diversity Rx antennas for lying scenarios in the ferry environment.

Scenario	Rx no.	Rx antenna placement	Upper berth			Lower berth		
			μ (dB)	$\lvert\delta\rvert$ (dB)	σ (dB)	μ (dB)	$\lvert\delta\rvert$ (dB)	σ (dB)
Lying on the back with hands along the body	Rx1	TO_F	58.7	2.9	4.7	62.5	8.2	6.6
	Rx2	TO_B	61.6		4.9	54.3		5.1
	Rx1	TO_F	50.8	8.3	4.0	50.4	2.5	4.2
	Rx2	AB_R	59.1		4.5	52.9		3.9
Lying on the front with hands under the head	Rx1	TO_F	61.4	10.0	4.7	58.5	6.1	4.3
	Rx2	TO_B	51.4		5.0	52.4		5.1
	Rx1	TO_F	53.4	6.7	4.1	63.4	1.5	4.2
	Rx2	AB_R	60.1		4.0	64.9		7.7
Lying on the left side with the right hand under the head	Rx1	TO_F	46.8	8.4	4.3	57.2	4.3	4.8
	Rx2	TO_B	55.2		4.9	61.5		5.7
	Rx1	TO_F	55.7	8.4	4.1	49.3	13.6	4.1
	Rx2	AB_R	64.1		3.8	62.9		4.3
Lying on the right side with the right hand under the head	Rx1	TO_F	66.5	10.8	4.7	50.1	10.2	4.3
	Rx2	TO_B	55.7		5.6	60.3		5.6
	Rx1	TO_F	57.2	0.2	4.4	52.0	1.6	4.1
	Rx2	AB_R	57.4		4.4	53.6		4.0

Table 4: The mean (μ) and standard deviation (σ) of system loss and the average XPD for different polarizations of the Rx antenna for walking scenarios in the ferry environment.

Walking scenario	Tx antenna placement	Rx no.	Rx antenna polarization	μ (dB)	σ (dB)	XPD (dB)
Approaching	HE_R	Rx1	H	45.9	7.2	2.8
		Rx2	V	43.1	6.8	
	TO_F	Rx1	H	45.0	7.3	9.0
		Rx2	V	36.0	7.1	
	AB_L	Rx1	H	46.2	7.5	5.5
		Rx2	V	40.7	6.6	
Departing	HE_R	Rx1	H	48.0	6.6	3.0
		Rx2	V	45.0	7.5	
	TO_F	Rx1	H	50.2	6.7	7.1
		Rx2	V	43.1	7.0	
	AB_L	Rx1	H	48.9	6.9	2.7
		Rx2	V	46.2	7.5	

in the same office environment as the one described in the section related to SL measurements for space diversity. As for the off-body Tx antenna, the linearly polarized UWB monopole antenna [18] has been chosen, while as for the on-body Rx antenna, the dual-polarized UWB antenna [21] has been used. The Tx antenna was attached to the wall on one side of the room at a height of 2 m in such a way as to obtain the vertical polarization. Among the large number of measured scenarios and antenna placements described in [35], only the approaching and departing walking scenarios with the on-body Rx antenna placed on TO_F have been presented in this study. In this case, the user was walking along the axis of the room, facing front and back to the Tx antenna.

The examples of Rx power delay distributions over time for the vertically and horizontally polarized on-body antenna have been shown in Figure 9. As of the case of the user departing from the Tx antenna, one can observe the weak direct path component as a result of body-shadowing from the user. However, some power is still received over this path, due to the creeping wave propagation around the body. Furthermore, in this case, the direct path delay is changing linearly. Additionally, some differences in Rx power distributions for orthogonal polarizations may be observed.

Figures 10–12 present the total Rx power, the average delay, and the r.m.s. delay spread, respectively, over time for V- and H-polarized on-body antennas for both approaching and departing scenarios. For each polarization, the scenario has been repeated 5 times. It may be observed that the total Rx power is changing according to time and is related to the change of the length of the radio wave propagation path and that the total power is typically higher for the vertical polarization (one has to remember that the Tx antenna was V-polarized). In contrast, the average delay for the approaching case is from the range of 4 ns up to 28 ns for both polarizations, while for departing, this range is wider, from 12 ns up to 33 ns, and the differences between both polarizations are not so apparent. Similarly, for the case of the r.m.s. delay spread, which is from 4 ns to 20 ns for approaching and from 7 ns to 18 ns for departing, these values are once better for the vertical polarization and once for the horizontal one. This shows that by using polarization diversity, one can select the polarized radio channel with temporarily better characteristics.

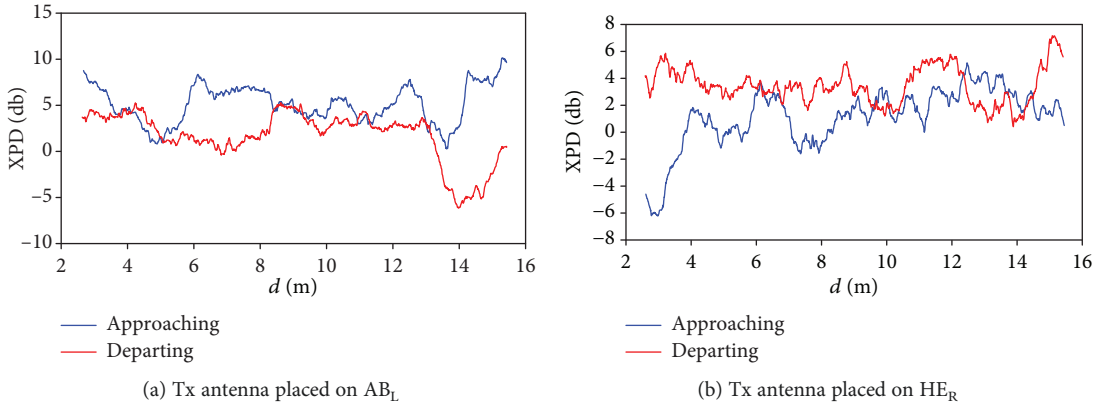

(a) Tx antenna placed on AB_L (b) Tx antenna placed on HE_R

FIGURE 7: XPD vs. length of the propagation path (d) for approaching and departing scenarios.

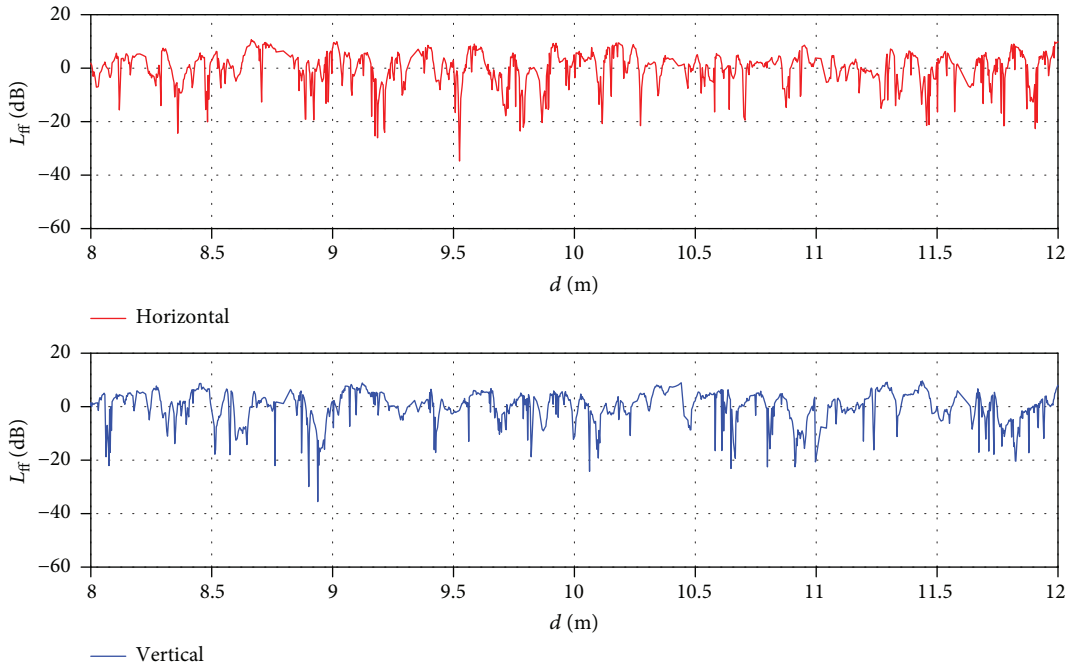

FIGURE 8: Magnitude of fast fading (L_{ff}) vs. sample length of the propagation path (d) for departing scenario and Tx antenna placed on TO_F.

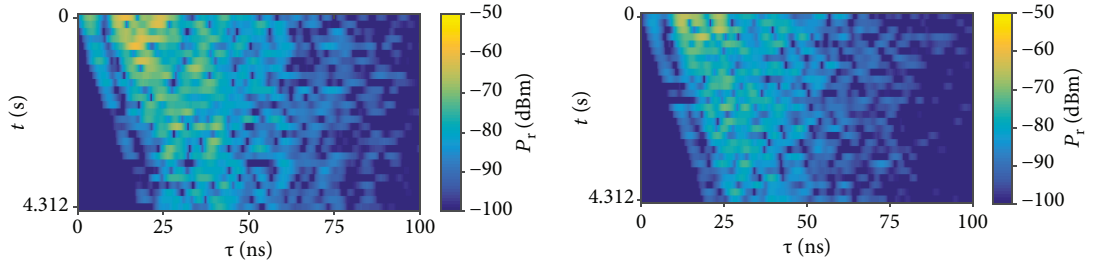

(a) (b)

FIGURE 9: Rx power (P_r) vs. delay (τ) and time (t), for the vertically (a) and horizontally (b) polarized on-body antenna placed on TO_F and the user departing scenario.

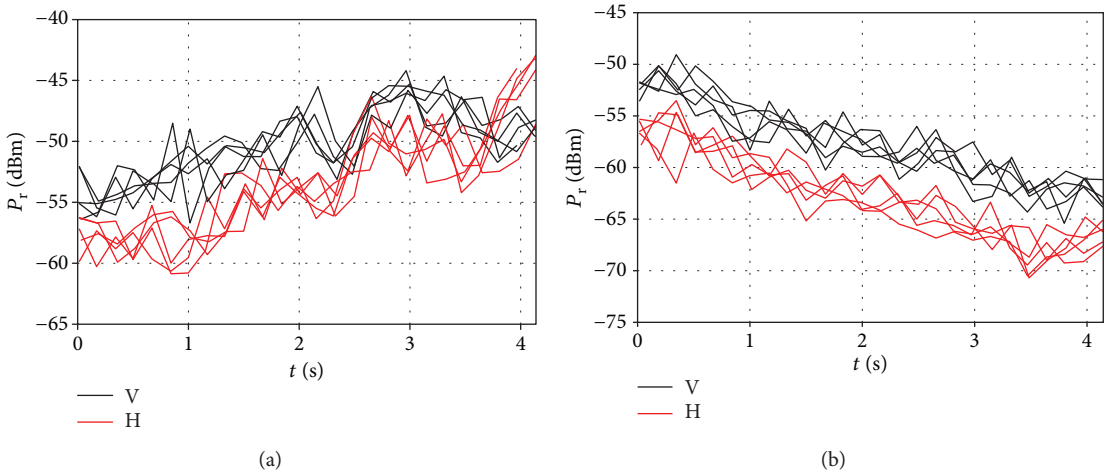

FIGURE 10: Total Rx power (P_r) vs. time (t), for the V- and H-polarized on-body antenna placed on TO_F and the user approaching (a) and departing (b) scenarios.

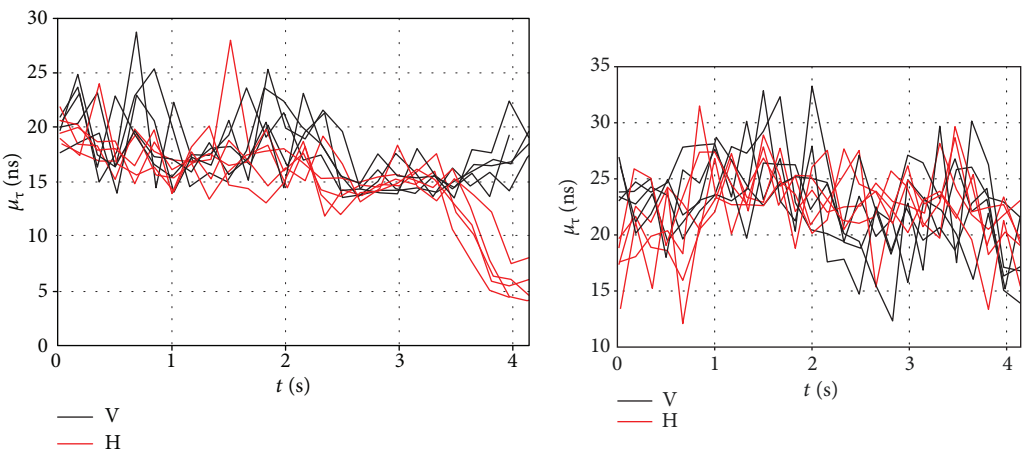

FIGURE 11: Average delay (μ_τ) vs. time (t), for the V- and H-polarized on-body antenna placed on TO_F and the user approaching (a) and departing (b) scenarios.

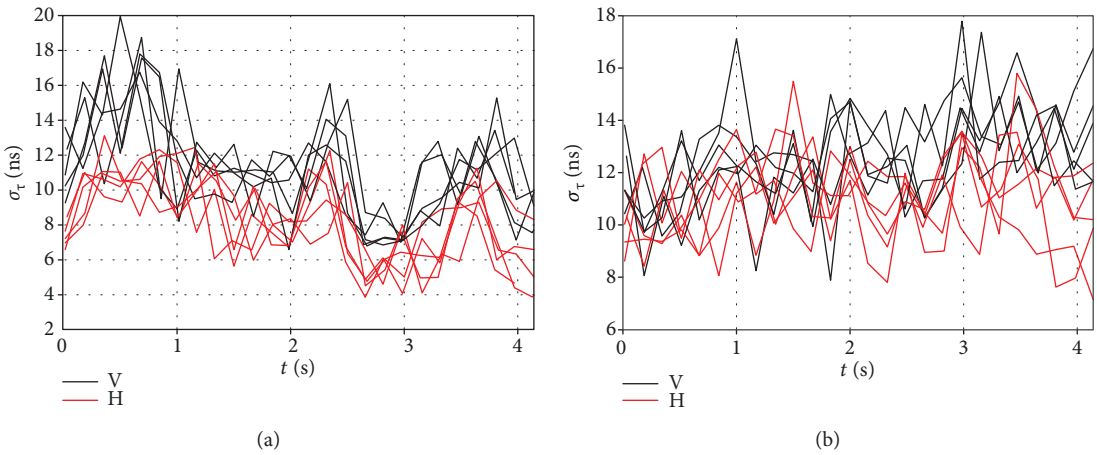

FIGURE 12: R.m.s. delay spread (σ_τ) vs. time (t), for the V- and H-polarized on-body antenna placed on TO_F and the user approaching (a) and departing (b) scenarios.

6. Conclusions

The general aim of the article was to present the versatile measurement stand, as well as the measurement methodology and scenarios being used during research carried out under the umbrella of COST Action CA15104 "Inclusive Radio Communication Networks for 5G and beyond" (IRACON) [4]. In addition, the presented measurement stand is a part of the map of research groups and laboratories in Europe (and close countries), the so-called "Map of Experts," organized within the EurAAP (European Association on Antennas and Propagation) Working Group on Propagation [36].

The concept of the experimental test bed for SL and CIR measurements for off-body and body-to-body radio channels in WBANs has been fully described. This test bed consists of the following sections: executive, RF switching, antennas, and control. The possible measurement scenarios that may occur in off-body and body-to-body channel investigation have been classified and described in detail. The considered classification includes the object of measurements, diversity scheme, mutual visibility of Tx and Rx antennas, environments, possible antennas' placement, mutual antenna orientation, and user motion. Additionally, the evaluation of the standard and expanded uncertainty of the presented measurement stand and methodology has been provided. In the last section, the exemplary results have been presented and discussed. These measurements consider SL measurements in off-body narrowband channels with a space diversity scheme for walking and lying scenarios in office and ferry environments. In addition, the experimental results consider SL and CIR for a polarization diversity scheme, in an off-body narrowband and an ultrawideband channel, respectively. The analysis of mean SL, magnitudes of fast fading, XPD, Rx power delay, average delay, and r.m.s. delay spread allows one to draw the conclusion that there is a need for further investigations of different diversity schemes and their applications in WBANs. The presented measurement stand and methodology are a perfect facility that may be used for this purpose.

Data Availability

The measurement data used to support the findings of this study are available from the corresponding author upon request.

Conflicts of Interest

The author declares that there is no conflict of interest regarding the publication of this paper.

Acknowledgments

The author would like to thank the joint research team of Gdansk University of Technology (Department of Radio Communication Systems and Networks) and University of Lisbon (Instituto Superior Tecnico) for the research work carried out jointly in the field of channel modeling in WBANs.

References

[1] T. G. Zimmerman, "Personal area networks: near-field intrabody communication," *IBM Systems Journal*, vol. 35, no. 3.4, pp. 609–617, 1996.

[2] Institute of Electrical and Electronics Engineers, "IEEE 802.15.6-2012 - IEEE standard for local and metropolitan area networks-part 15.6: wireless body area networks," 2012, https://standards.ieee.org/standard/802_15_6-2012.html.

[3] A. Reichman and J. Takada, "Body communications," in *Pervasive Mobile & Ambient Wireless Communications*, R. Verdone and A. Zanella, Eds., Springer, London, UK, 2012.

[4] October 2018, http://www.iracon.org/.

[5] C. Ahn, B. Ahn, S. Kim, and J. Choi, "Experimental outage capacity analysis for off-body wireless body area network channel with transmit diversity," *IEEE Transactions on Consumer Electronics*, vol. 58, no. 2, pp. 274–277, 2012.

[6] P. T. Kosz, S. J. Ambroziak, and L. M. Correia, "Radio channel measurements in off-body communications in a ferry passenger cabin," in *2017 XXXIInd General Assembly and Scientific Symposium of the International Union of Radio Science (URSI GASS)*, pp. 1–4, Montreal, QC, Canada, August 2017.

[7] T. Aoyagi, J.-i. Takada, K. Takizawa et al., "Propagation characteristics for 2.45 GHz dynamic wearable WBAN using multiport VNA," in *2012 6th International Symposium on Medical Information and Communication Technology (ISMICT)*, pp. 1–4, La Jolla, CA, USA, March 2012.

[8] L. Liu, V. Bhatnagar, C. G. Robles, P. De Doncker, L. Vandendorpe, and C. Oestges, "Investigation of channel spatial diversity for dual-link cooperative communications in WBAN," in *Proceedings of the 5th European Conference on Antennas and Propagation (EUCAP)*, pp. 2972–2976, Rome, Italy, April 2011.

[9] K. Turbic, S. J. Ambroziak, and L. M. Correia, "Characteristics of the polarised off-body channel in indoor environments," *EURASIP Journal on Wireless Communications and Networking*, vol. 2017, 2017.

[10] L. Liu, P. De Doncker, and C. Oestges, "Fading correlation measurement and modeling on the front side of a human body," in *2009 3rd European Conference on Antennas and Propagation*, pp. 969–973, Berlin, Germany, March 2009.

[11] M. Kim, K. Wangchuk, and J. Takada, "Link correlation property in WBAN at 2.4 GHz by multi-link channel measurement," in *2012 6th European Conference on Antennas and Propagation (EUCAP)*, pp. 548–552, Prague, Czech Republic, March 2012.

[12] D. Goswami, K. C. Sarma, and A. Mahanta, "Experimental determination of path loss and delay dispersion parameters for on-body UWB WBAN channel," in *2015 IEEE International Conference on Signal Processing, Informatics, Communication and Energy Systems (SPICES)*, pp. 1–4, Kozhikode, India, February 2015.

[13] M. Hämäläinen, T. Kumpuniemi, and J. Iinatti, "Observations from ultra wideband on-body radio channel measurements," in *2014 XXXIth URSI General Assembly and Scientific Symposium (URSI GASS)*, pp. 1–4, Beijing, China, August 2014.

[14] T. Kumpuniemi, T. Tuovinen, M. Hämäläinen, K. Y. Yazdandoost, R. Vuohtoniemi, and J. Iinatti, "Measurement-based on-body path loss modelling for UWB WBAN communications," in *2013 7th International Symposium on Medical Information and Communication Technology (ISMICT)*, pp. 233–237, Tokyo, Japan, March 2013.

[15] K. K. Cwalina, S. J. Ambroziak, P. Rajchowski, and L. M. Correia, "Radio channel measurements in 868 MHz off-body communications in a ferry environment," in *2017 XXXII General Assembly and Scientific Symposium of the International Union of Radio Science (URSI GASS)*, pp. 1–4, Montreal, QC, Canada, August 2017.

[16] S. J. Ambroziak, L. M. Correia, and K. Turbic, "Radio channel measurements in body-to-body communications in different scenarios," in *2016 URSI Asia-Pacific Radio Science Conference (URSI AP-RASC)*, pp. 1376–1379, Seoul, South Korea, August 2016.

[17] T. Kumpuniemi, M. Hämäläinen, K. Y. Yazdandoost, and J. Iinatti, "Measurements for body-to-body UWB WBAN radio channels," in *2015 9th European Conference on Antennas and Propagation (EuCAP)*, pp. 1–5, Lisbon, Portugal, April 2015.

[18] M. Koohestani, N. Pires, A. K. Skrivervik, and A. A. Moreira, "Influence of the human body on a new coplanar-fed ultra-wideband antenna," in *2012 6th European Conference on Antennas and Propagation (EUCAP)*, Prague, Czech Republic, March 2012.

[19] D. Gaspar, *Project and study of a belt antenna*, Master's thesis, Instituto Superior Tecnico (IST), University of Lisbon, 2009, https://fenix.tecnico.ulisboa.pt/downloadFile/395139412940/resumo.pdf.

[20] *A-Info, LB-OSJ_0760, 0.7-6.0GHz Open Boundary Quad-Ridged Horn*, http://www.ainfoinc.com/en/pro_pdf/new_products/antenna/Dual%20Polarization%20Horn%20Antenna/tr_LB-OSJ-0760.pdf.

[21] T. Pinto and A. A. Moreira, *UWB antenna design for diversity scenarios*, MSc thesis summary, Instituto Superior Tecnico (IST), University of Lisbon, Tech. Rep., 2015, https://fenix.tecnico.ulisboa.pt/downloadFile/281870113702347/Extended Abstract.pdf.

[22] J. Ferreira, *Study and design of antennas for WLAN MIMO applications*, MSc thesis summary, Instituto Superior Tecnico (IST), University of Lisbon, Tech. Rep., 2016, https://fenix.tecnico.ulisboa.pt/downloadFile/1407770020545444/ExtendedAbstract.pdf.

[23] ITU-R P 341-6, *The Concept of Transmission Loss for Radio Links*, International Telecommunication Union – Radiocommunication Sector, 2016.

[24] ITU-R P 310-9, *Definitions of Terms Relating to Propagation in Non-Ionized Media*, International Telecommunication Union – Radiocommunication Sector, 1994.

[25] ITU-R P 1407-6, *Multipath Propagation and Parameterization of Its Characteristics*, International Telecommunication Union – Radiocommunication Sector, 2017.

[26] J. Sadowski, "Measurement of coherence bandwidth in UHF radio channels for narrowband networks," *International Journal of Antennas and Propagation*, vol. 2015, Article ID 985892, 11 pages, 2015.

[27] S. Salous, *Radio Propagation Measurement and Channel Modelling*, Wiley, 2013.

[28] S. J. Ambroziak, L. M. Correia, R. J. Katulski et al., "An off-body channel model for body area networks in indoor environments," *IEEE Transactions on Antennas and Propagation*, vol. 64, no. 9, pp. 4022–4035, 2016.

[29] M. Mackowiak, *Modelling MIMO systems in body area networks in outdoors*, Ph. D. Dissertation, IST-University of Lisbon, Lisbon, Portugal, 2013.

[30] M. Mackowiak and L. M. Correia, "Modelling dynamic body-to-body channels in outdoor environments," in *2014 XXXIth URSI General Assembly and Scientific Symposium (URSI GASS)*, pp. 1-2, Beijing, China, August 2014.

[31] S. J. Ambroziak, L. M. Correia, R. J. Katulski, and M. Maćkowiak, "Impact of radio wave polarisation on off-body communications in indoor environments," in *2015 9th European Conference on Antennas and Propagation (EuCAP)*, pp. 1–3, Lisbon, Portugal, April 2015.

[32] JCGM 100: 2008, *Evaluation of Measurement Data — Guide to the Expression of Uncertainty in Measurement, First Edition*, Joint Committee for Guides in Metrology, 2008.

[33] S. Wiszniewski and S. J. Ambroziak, "System loss analysis in body area networks with space diversity scheme," in *2018 Baltic URSI Symposium (URSI)*, pp. 51-52, Poznan, Poland, May 2018.

[34] October 2018, https://www.lsr.com/downloads/products/330-0149.pdf.

[35] K. Turbic, S. J. Ambroziak, L. M. Correia, and M. Beko, "Wide-band channel measurements for polarised indoor off-body communications," in *IRACON 7th MC meeting and 7th Technical meeting, Technical document: TD(18)07063*, Cartagena, Spain, May-June 2018.

[36] November 2018, http://www.euraap.org/Activities/wg/detailed-presentation-for-each-wg/propagation.